KICS The Korean Institute of Communications and Information Sciences

Available online at www.sciencedirect.com

ScienceDirect

ICT Express xxx (xxxx) xxx

www.elsevier.com/locate/icte

A Survey and analysis on a troposcatter propagation model based on ITU-R recommendations

In-Seok Lee[a], Jung-Hoon Noh[b], Seong-Jun Oh[c,*]

[a] *Department of Computer Science and Engineering, Korea University, Seoul, Republic of Korea*
[b] *Electronic Engineering, Kumoh National Institute of Technology, Gumi, Republic of Korea*
[c] *Graduate School of Information Security, Korea University, Seoul, Republic of Korea*

Received 1 May 2022; received in revised form 30 August 2022; accepted 16 September 2022
Available online xxxx

Abstract

Signal scattering in the troposphere is a phenomenon referred to as "troposcatter", and it is promising method for wireless communication beyond the line of sight (b-LOS). For a troposcatter communication system, it is important to develop a channel model for the tropospheric scatter. Recently, b-LOS communication using troposcatter received much attention for its application to military communication. Thus, a comprehensive review and analysis of conventional ITU-R troposcatter propagation models and recent results would be a timely study. Accordingly, in this study, we analyze and simulate the tropospheric scatter propagation model proposed by the ITU-R. Troposcatter propagation models in ITU-R recommendations consist of three parts: basic transmission loss, gaseous absorption, and a precipitation fading model. The ITU-R P.2001 simulation model shows basic transmission losses of 210 dB and 240 dB at 0.2 GHz and 2 GHz in 300 km distances, respectively. The ITU-R P.452 model results in 20 dB less loss, but this is dependent on measurement conditions. Gaseous absorption and precipitation fading have less than 1 dB loss for frequencies less than 2 GHz, but can increase to be over 10 dB in loss for frequencies of 2 GHz and above. We also review recent studies on tropospheric scatter channel models and communication systems. In addition to these reviews, we examine recent studies on ray tracing methods for tropospheric scatter channel models.

Keywords: Troposcatter; Communication; Propagation model; Transmission loss prediction

Contents

* Corresponding author.
E-mail addresses: insukee@korea.ac.kr (I.-S. Lee), jhnoh@kumoh.ac.kr (J.-H. Noh), seongjun@korea.ac.kr (S.-J. Oh).
Peer review under responsibility of The Korean Institute of Communica-
https://doi.org/10.1016/j.icte.2022.09.009

Please cite this article as: I.-S. Lee, J.-H. Noh and S.-J. Oh, A Survey and analysis on a troposcatter propagation model based on ITU-R recommendations, ICT Express (2022), https://doi.org/10.1016/j.icte.2022.09.009.

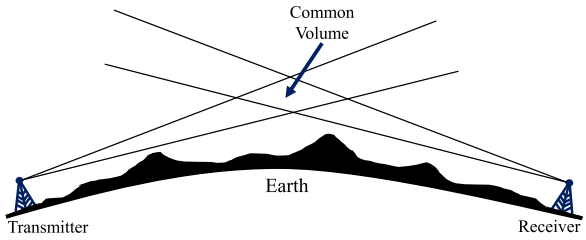

Fig. 1. Tropospheric scatter communication.

1. Introduction

Tropospheric scattering (troposcatter) denotes a phenomenon of signal scattering caused by atmospheric irregularities in the troposphere. Troposcatter communication denotes a promising candidate for beyond line-of-light(b-LOS) wireless communication method based on the troposcatter of signals [1–5].

Fig. 1 illustrates the case of b-LOS communication, where the transmitter and receiver are far apart. The transmitter sends the signal toward the troposphere so as not to be blocked by terrestrial obstacles. Although most of the transmitted signal passes out of the troposphere, some of it scatters at the troposphere, which we call "common volume".

To use the troposcatter for communication, as shown in Fig. 1, an antenna facing a horizontal line should be placed, and the elevation angle of the antenna should be as low as possible to minimize the path length. As shown in Fig. 1, a common volume is formed at the intersection of the antenna beam-widths, and the receiver receives scattered radio waves from this area.

Troposcatters were discovered in the 1930s and developed in the 1950s for over-the-horizon b-LOS communications [6]. At that time, a troposcatter was the only feasible method for direct wireless communication of up to 300 km. However, troposcatter communication was considered expensive, as large parabolic reflector antennas and high-power amplifiers were essential owing to the large propagation loss [7]. Since the 1970s, satellite communication (SATCOM) has been developed and used for b-LOS communication as an economical solution. With this low cost approach, b-LOS troposcatter communications have mostly been replaced by SATCOMs [8].

However, with further development in antenna technology, the drawbacks of troposcatters have also been addressed. [9] studies the antenna suitable for long distance communication, in parallel with developments for compact and low-profile antenna that reduces in size [10–12]. Owing to the developments in antenna and amplifier equipment, it is possible to resolve the large propagation loss issue by providing sufficient transmit power at a low cost. Since troposcatter equipment is sufficiently small to be transported by a truck, it has the advantage of being easily installed and moved to the desired location. Troposcatters also have additional advantages over SATCOM. For example, SATCOM has very high transmission delays of over 500 ms, whereas troposcatter communication has low transmission delays of a few milliseconds [7]. Since SATCOM covers a large area, it is easily exposed to jamming and can cause security problems; however, a troposcatter communication system is more robust than SATCOM in terms of security because it uses narrow-beam antennas and provides a point-to-point communication link [6,7,13]. In addition to these applications, troposcatter communication can be applied to time synchronization and over-the-horizon detection and positioning [14]. Given the increasing importance of security and low transmission delay, the troposcatter has become a promising candidate for b-LOS communication. Recently, the NATO IST-172 research task group has been investigating non-satellite and non-high frequency methodologies for b-LOS communication, and is considering troposcatter communication for atmospheric relays [15].

To utilize the troposcatter phenomenon for over-the-horizon communication, it is essential to develop an appropriate troposcatter propagation model for predicting transmission loss. However, troposcatter model development is not an easy task, given that the troposcatter transmission loss has a large range of fluctuations depending on terrain, atmospheric conditions, weather, and other factors. Moreover, it is a challenging task to measure propagation losses in a long distance. To obtain reliable measurement data, it is necessary to measure the propagation loss for more than one year at various locations worldwide. Therefore, theoretical studies were conducted in the early days [3]. The theory of signal scattering caused by air turbulence was proposed by [16] in 1950, the coherent reflection theory was proposed by [17] in 1953, and the theoretical model of reflection for over-the-horizon propagation was proposed by [18] in 1957. Since the 1980s, the International Telecommunication Union Radiocommunication Sector (ITU-R) has collected measurement data worldwide, created a data bank [19], and used it to make recommendations on standardized troposcatter loss prediction methods [20].

Recently, based on the propagation model of the ITU-R recommendations, studies have been conducted to reinforce or develop the ITU-R model more accurately through an optimization algorithm. In addition, new troposcatter channel models are proposed based on the past theoretical model, and a modeling approach using ray-tracing and parabolic equations is also being studied. In this study, we analyze troposcatter propagation model recommended by the ITU-R and review recent research on troposcatter channel model.

The remainder of this paper is organized as follows. In Section 2, we analyze the three troposcatter models recommended by ITU-R and predict troposcatter transmission losses through simulations. Section 3 introduces and reviews further research on the troposcatter model, and Section 4 concludes the paper.

2. ITU-R recommendations

2.1. Long distance propagation model

ITU-R is an international union created to ensure the rational usage of the radio frequency spectrum, and standardize the technical characteristics and frequency use of wireless communication services and systems. In particular, ITU-R provides long-distance radio wave propagation model recommendations for cases in which wireless communication radio

waves are transmitted over very long distances. Three long-distance propagation model recommendations are provided by ITU-R: P.452, P.2001, and P.617.

The ITU-R P.452-17 recommendation is a model for evaluating radio interference on Earth's surface [21]. It is used to estimate the radio wave interference between communication systems sharing the same or adjacent frequency bands. For the interference evaluation, the P.452 model assumes the worst case. It is mainly used to estimate the interference for 0.001% to 50% of the "time percentage", i.e., the percentage of the average year for which the predicted transmission loss is not exceeded. The result of prediction using the ITU-R model is shown as a distribution of transmission loss over one year.

The ITU-R P.617-5 recommendation is a propagation model for trans-horizon radio-relay systems [22]. The model proposes the data and propagation prediction techniques required for the design of a radio relay system beyond the horizon, as well as a transmission loss prediction model for troposcatter signals. Many changes have been made since the P.617 recommendation was first proposed in 1992. From P.617-1 in 1992 to P.617-3 in 2013, this model was mainly used to predict the performance of a radio relay system from 50% to 99.999% of the time percentage. As it was updated to P.617-4 in 2017 and P.617-5 in 2019, i.e., the latest version of this recommendation, the model was improved to predict performance for a time percentage of 0.001% to 99.999%.

The ITU-R P.2001-4 recommendation is a wide-range propagation model used for general purposes [23]. In its first publication in 2013, P.2001 included the propagation models of both P.452-15 and P.617-3 to provide a wide-range propagation model able to be used for more general purposes, with a model for predicting the propagation loss for a time percentage of 0.001% to 99.999% [20]. Compared to P.452 for interference evaluation or P.617 for radio-relay systems, P.2001 can be used to predict the transmission losses for long-distance radio waves. Additionally, because the path attenuation equations are modularized through independent sub-models, P.2001 is better suited for computer simulations such as Monte Carlo simulations. In particular, P.2001 proposes a climate zone table in relation to the troposcatter model to consider the attenuation of the common volume according to the latitude and longitude of the transceiver. The parameter values related to the meteorological and atmospheric conditions are determined according to the climate zone table.

A comparison of the ITU-R long-distance channel model configurations is presented in Table 1. As the range of frequencies or distances to which each model can be applied is different, reliable results can only be obtained when the appropriate model is applied to the desired experimental environment. Antenna altitude in P.2001 is mentioned to be up to 8000 m, but other models do not mention it; similarly, the common volume's latitude and longitude is only estimated in P.2001. A digital map provides data in a manner such that the value of a variable can be selected according to the latitude and longitude of the experimental environment. Refractivities in the lowest 1 km, in the lowest 65 m, and at sea-level represent the refractivity values of each altitude, respectively. The variable for the rainfall rate references M_t (annual rainfall accumulation), P_{r6} (Probability for rain in the next 6 h), and β (ratio between convective and total precipitation) [24,25]. FoE refers to the critical sporadic E frequency. As it is a map based on actual measurement data, it can be used reliably and conveniently. For example, when using the channel model for P.2001, the value of refractivity at the lowest 1 km can be selected from the map and entered according to the latitude and longitude of the experimental environment. However, since a digital map is not provided in P.452, the refractivity value for the experimental environment must be directly measured and entered. The P.2001 model classifies seven climate zones (one of them is the sea path) according to the latitude and longitude, and each climate zone has its own meteorological and atmospheric structure parameters.

The propagation mechanisms commonly mentioned in the above recommendations are surface diffraction, ducting, and troposcatter. Surface diffraction refers to diffraction by topography, whereas ducting refers to the propagation of radio waves as reflection and refraction are repeated from the atmospheric layer formed on the ground. Among these, troposcatter is the only propagation mechanism that can be used in long-distance communication systems. Diffraction is strongly influenced by terrain, whereas ducting mostly occurs over sea/water or flat coastal land areas, and is difficult to predict because of the highly sensitive radio refractivity. However, troposcatter is unaffected by topography, and energy transmission through the common volume is relatively easy. The scattered energy can be reliably be received at a receiver by pointing narrow-beam antennas toward the common volume.

2.2. Troposcatter propagation model

The troposcatter propagation model recommended by ITU-R consists of three parts: basic transmission loss, gaseous absorption, and precipitation fading, as follows:

$$L_{TP} = L_{bs} + L_g + L_p. \quad (1)$$

In the above, L_{TP} is the troposcatter loss, L_{bs} is the basic transmission loss, L_g is the gaseous absorption loss, and L_p is the precipitation fading. The log-domain sum of the three transmission loss calculations provides the total path loss owing to troposcatter. The basic transmission loss refers to the amount of transmission loss caused by the frequency, distance between transmitter/receiver, antenna gain, terrain profile, refractive index, etc. Precipitation fading refers to the transmission loss in a rainfall situation, whereas gaseous absorption is caused by atmospheric conditions (such as the density of the water vapor in the atmosphere).

The troposcatter model equation of P.2001 considers all three losses, i.e., the basic transmission loss, precipitation fading, and gaseous absorption. The troposcatter model equation in P.452 considers the basic transmission losses and gaseous absorption. The troposcatter model equation in P.617 considers only the basic transmission loss. It can be seen that the troposcatter model in P.2001 presents a model that can be used more generally, including in various attenuation causes.

Table 1
Comparison of International Telecommunication Union Radiocommunication Sector (ITU-R) long-distance channel model configuration.

Parameters		P.2001-4	P.452-17	P.617-5
Frequency		30 MHz to 50 GHz	0.1 GHz to 50 GHz	Above 30 MHz
Antenna altitude		Up to 8000 m	–	–
Common volume location estimation		O	X	X
Time percentage		0.001∼99.999	0.001∼50	0.001∼99.999
Distance		3 km to 1000 km	Up to 10 000 km	–
Digital maps	Refractivity in the lowest 1 km	O	X	O
	Refractivity in the lowest 65 m	O	X	X
	Sea-level surface refractivity	X	X	O
	Variable for rainfall rate	O	X	X
	Surface water-vapor density	O	X	X
	Troposcatter climate zone	O	X	X
	FoE	O	X	X

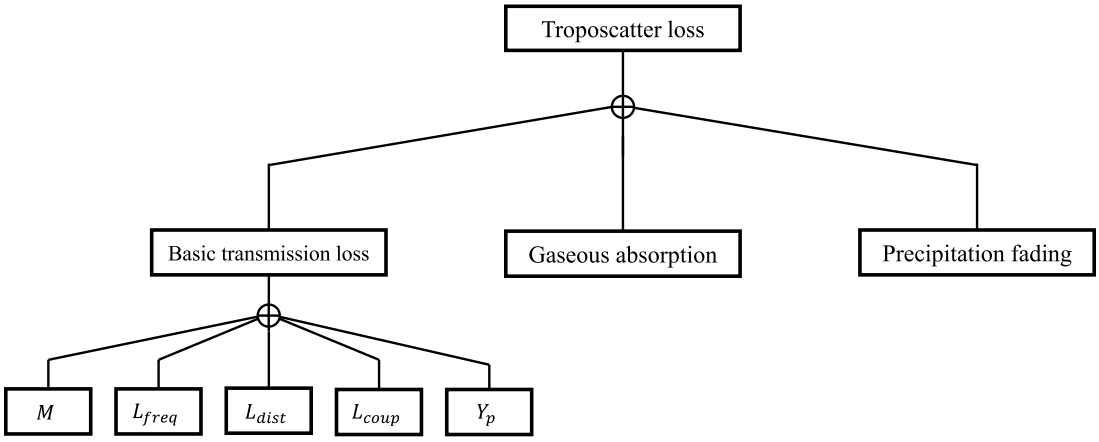

Fig. 2. The diagram of the ITU-R troposcatter loss model.

A common equation for the basic transmission loss equation is given as follows:

$$L_{\text{bs}} = M + L_{\text{freq}} + L_{\text{dist}} + L_{\text{coup}} - Y_{\text{p}}. \tag{2}$$

Here, M is a meteorological parameter; L_{freq} is the loss determined by the frequency; L_{dist} is the loss determined by the transmission distance, scattering angle, etc.; L_{coup} is the loss determined by the antenna gain; and Y_{p} is the loss determined by the time percentage. Fig. 2 explains the troposcatter propagation model in the ITU-R recommendation, where (1) and (2) are pictorially illustrated.

The detailed expressions for the basic transmission loss in P.2001 are as follows:

$$L_{\text{freq, P.2001}} = 25\log(f) - 2.5[\log(0.5f)]^2, \tag{3}$$

$$L_{\text{dist, P.2001}} = \max[10\log(d) + 30\log(\theta) + L_{\text{N}}, \; 20\log(d) + 0.573\theta + 20], \tag{4}$$

and

$$L_{\text{coup, P.2001}} = 0.07\exp[0.055(G_t + G_r)], \tag{5}$$

where f represents the frequency, d is the transmission distance θ is the scattering angle, G_{t} is the transmit antenna gain, L_{N} is a loss term dependent on the common volume height, and G_{r} is the gain of the receiving antenna. If a climate zone matching the latitude/longitude of the communication environment in the climate zone map is chosen, the M and Y_p values can be obtained.

The detailed equations for the basic transmission loss in P.452 are as follows:

$$L_{\text{TP, P.452}} = 190 + L_{\text{freq}} + L_{\text{dist, P.452}} - 0.15N_0 + L_{\text{coup}} + L_{\text{g}} - 10.1[-\log(p/50)]^{0.7}, \tag{6}$$

$$L_{\text{freq, P.452}} = 25\log(f) - 2.5[\log(f/2)]^2, \tag{7}$$

$$L_{\text{dist, P.452}} = 20\log(d) + 0.573\theta, \tag{8}$$

and

$$L_{\text{coup, P.452}} = 0.051\exp[0.055(G_{\text{t}} + G_{\text{r}})], \tag{9}$$

where N_0 refers to the sea-level surface refractivity in the middle of the troposcatter communication path, and p is the time percentage.

Compared with the basic transmission loss model of P.2001, in P.452 L_{freq} is the same, but there is a difference between L_{dist} and L_{coup}. In a situation with the same transmit/receive antenna gain and distance, the model in P.2001 predicts a larger loss. This difference is attributed to P.452's assumption of the worst-case scenario.

The detailed equations in the troposcatter model in P.617 are as follows:

$$L_{\text{TP, P.617}} = F + L_{\text{freq, P.617}} + L_{\text{dist, P.617}} L_{\text{coup}-y_{\text{p}}}, \quad (10)$$

$$L_{\text{freq, P.617}} = 22\log(f), \quad (11)$$

$$L_{\text{dist, P.617}} = 17\log(d) + 35\log(\theta), \quad (12)$$

$$L_{\text{coup, P.617}} = 0.07\exp[0.055(G_{\text{t}} + G_{\text{r}})], \quad (13)$$

and

$$F = 0.18 \cdot N_0 \cdot \exp(-h_{\text{s}}/h_{\text{b}}) - 0.23 \cdot dN, \quad (14)$$

where N_0 represents the average annual sea level surface refractivity, and dN represents the average annual radio-refractive index lapse rate through the lowest 1 km of the atmosphere. N_0 and dN are determined according to the latitude and longitude of the communication link, respectively. h_{s} represents the height of the Earth's surface above sea level. h_{b} refers to the scale height and can be determined statistically for different climatic conditions, with a global mean of 7.35 km.

From comparing P.617 with the basic transmission loss in P.2001, it can be seen that the loss owing to the antenna gain is the same, whereas there are differences in the coefficients for the loss owing to the distance, scattering angle, and frequency. The reason for these differences is discussed in [20], which is reviewed in Section 3.

The attenuation by gas absorption is modeled in P.2001 and P.452. The gas absorption in P.452 refers to the ITU-R P.676 recommendation and is modeled as a function of the water vapor density ρ and transmission distance d. The gaseous absorption modeling in P.2001 is different from the calculation process in P.676, but there is a limiting condition for P.2001 which invalidates the model for frequency bands above 54 GHz. Therefore, P.676 is a more general formula. The specific attenuation owing to the air condition γ is determined by the frequency and water vapor density. The value of the water vapor density is selected from a table in P.2001, and determined by the latitude/longitude. Detailed gaseous absorption formulas can be found in P.2001 (attachment F), and are omitted in this paper.

The precipitation fading of the troposcatter is only modeled for P.2001. The loss from precipitation fading is determined by various factors such as the ratio of the distance from the transmitter to the scattering volume and distance from the scattering volume to the receiver, height, latitude/longitude, and precipitation. Detailed precipitation formulas can also be found in P.2001 (attachment C), and are omitted herein. P.452 uses, a hydrometeor-scatter interference prediction model, as the troposcatter model assumes a clear air propagation environment.

In addition to the above three long-distance channel model recommendations, other ITU-R recommendations may be related to the troposcatter channel model. Several P-series documents related to the ITU-R meteorological environment model are briefly reviewed and summarized in Table 2.

2.3. Model simulation

The ITU-R provides source code for implementing the long-distance propagation models of P.2001 and P.452 in MATLAB through the ITU-R SG3 data bank. In this study, we predicted the troposcatter loss in a real environment using the source code for P.2001 and P.452. In the same environment, the difference between the prediction of the troposcatter loss of the P.2001 and P.452 model is investigated through simulation. In addition, we examine the effect of gaseous absorption and precipitation fading. The simulation configurations are presented in Table 3, and the simulation environment is the same as the link number 908 in [19].

The cumulative distribution functions (CDFs) of the troposcatter propagation loss in the 0.2 GHz and 2 GHz frequency bands are shown in Fig. 3. The dotted line represents the result of P.452, and the solid line represents the result of P.2001. The x-axis represents the loss value, and the y-axis represents the time percentage. The CDF of the dotted line is displayed only up to 50% because the P.452 model can only provide a time percentage of up to 50%. In all frequency bands, the result for P.452 has less loss than that of P.2001. The difference is attributed to P.452 being a worst-case model in which interference waves are received; thus, the loss appears to be less than that of P.2001, which is a general-purpose model. Since the P.452 model assumes that interference signals are received through the troposphere, a low propagation loss denotes strong interference. Notably, in the results of both P.2001 and P.452, the loss increases at higher frequencies.

The effect of the loss owing to gas absorption and precipitation fading in the P.2001 model is shown in Fig. 4. The dotted line represents the basic transmission loss of the troposcatter, and the solid line represents the total sum of the basic transmission loss, gas absorption loss, and precipitation fading. The x-axis represents the loss value, and the y-axis represents the time percentage. The gas absorption loss is represented by adding a constant value regardless of the time percentage and is affected by the distance, frequency band, and water vapor density. In the low-frequency band of 2 GHz, the gas absorption loss is low, at approximately 1 dB. In contrast, in the high-frequency band of 30 GHz, the troposcatter loss is affected by approximately 10 dB.

As can be seen from the CDF with a time percentage of more than 90% in the 30 GHz band in Fig. 4, the loss increases rapidly. This is owing to the fading of precipitation. Fig. 5 shows the output of precipitation fading only in the troposcatter model of P.2001. The dotted line represents the loss at 30 GHz and the solid line represents the loss at 2 GHz. The x-axis represents the loss value, and the y-axis represents the time percentage. In the 2 GHz band, most losses from precipitation fading are 0 dB. This loss increases rapidly when the time frequency is 90% or more or in the high-frequency band of 30 GHz. Thus, when precipitation is severe, the high-frequency band is significantly affected.

Table 2
ITU P-series document summary.

Document number	Summary
453 [26]	The radio refractive index calculation method, required for long-distance channel model implementation, already referenced in P.2001
618 [27]	Prediction methods for Earth to space communication systems. It is expected to be more suitable for the channel model related to the satellite communication.
676 [28]	The document about attenuation by atmosphere gas, P.2001 and P.452 refer to it already.
835 [29]	Reference standard atmosphere. Statistical data in this document can be used when there is no measurement value for atmospheric conditions such as temperature/atmospheric pressure
840 [30]	The document about attenuation due to cloud and fog. It is expected to be more suitable for the channel model related to the satellite communication.
1144 [31]	The guideline for the propagation model of ITU-R Study Group 3

Table 3
Simulation configuration.

Parameter	Value	Unit
Frequency	0.2, 2, 30	GHz
Distance	301.87	km
Tx antenna gain	47.5	dBi
Rx antenna gain	47.5	dBi
Tx antenna height above ground	9.1	m
Rx antenna height above ground	2.7	m
Tx latitude [−90, +90]	40.3919	deg
Tx longitude [0, 360]	285.8131	deg
Rx latitude [−90, +90]	41.54	deg
Rx longitude [0, 360]	289.0689	deg

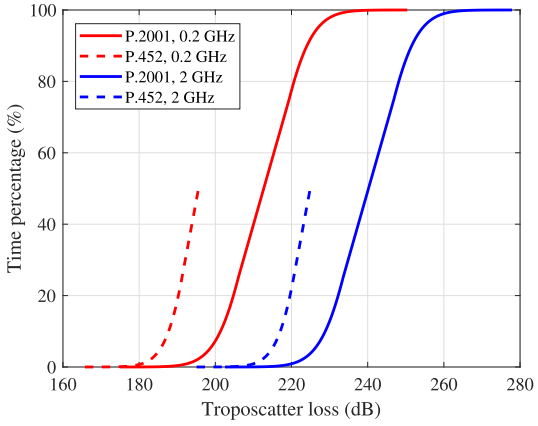

Fig. 3. Troposcatter loss cumulative distribution function (CDF) of International Telecommunication Union Radiocommunication Sector (ITU-R) P.2001 and P.452 models.

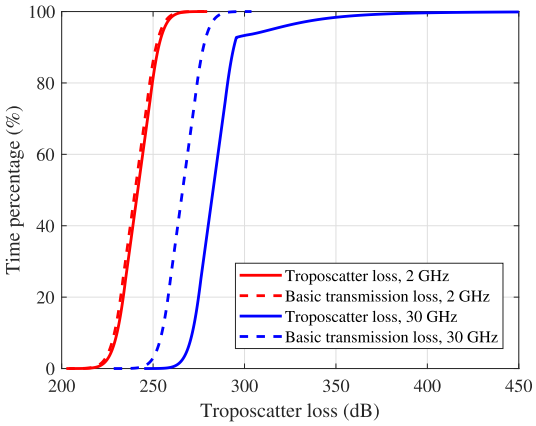

Fig. 4. Effect of gaseous absorption and precipitation fading in ITU-R P.2001 model.

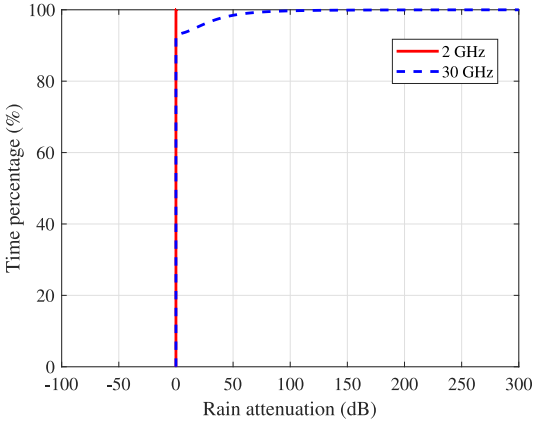

Fig. 5. Precipitation fading CDF of ITU-R P.2001 model.

3. Further research and application

3.1. Further study on the ITU-R model

In this subsection, further research on the ITU-R propagation model is reviewed.

In [20], ITU P.617, P.2001, and P.452 were combined to propose a new troposcatter transmission loss model. The authors introduced three channel models to find the propagation path parameters affecting the troposcatter transmission loss. The propagation parameters were the frequency, scatter angle, path length, and meteorological parameters (such as refractivity). Moreover, using the measured data of the Consultative Committee on International Radio (CCIR) data bank, the correlations between the transmission loss and propagation parameters were analyzed to set the range of the correlation coefficient x. Finally, the correlation coefficient x value was determined through genetic algorithm optimization, and a general equation that integrated the three models (P.617, P.2001,

and P.452) was derived. The mean value and root mean square error of the new proposed model were compared against those of the three independent ITU-R models; the new model was observed to have smaller prediction errors than the ITU-R models. The P.617-3 model referred to in [20] is the legacy model, and the new proposed model has been applied in the latest version, P.617-5.

In [32], the authors derived the troposcatter deviation loss for over-the-horizon(OTH) microwave propagation. The troposcatter loss predictions of the ITU-R recommendations did not consider this deviation loss. Instead, the procedure was as follows. First, the general parameters and path geometry of the troposcatter OTH propagation path were defined. Then, the deviation losses were derived by assuming Gaussian antenna patterns, based on a scatter transfer function. Finally, the deviation loss was divided into the azimuthal and vertical directions. For theoretical deviation analysis and verification, comparisons with the measurement data in [33,34] were performed.

In [35], a rain attenuation model was developed for troposcatter communications considering both the distribution of the rainfall rates and multiple rain cells. The rain attenuation model of the ITU-R recommendations is a rectangular rain cell having a uniform rainfall distribution. But in real world, distribution of rainfall rate shows significant changes. By modifying the HYCELL model [36], rain path length expressions for non-uniform rainfall distributions were proposed, and the rain loss owing to each rain cell was calculated. The rectangular rain cell model of ITU-R P.452 was also shown for as a comparison purposes. Through this simulation, it was shown that the effect of the rain loss is small at 4.7 GHz, but is large at 15 GHz.

3.2. Theoretical model

This subsection reviews studies on the troposcatter channel model and loss prediction model based on theoretical troposcatter model. These claim that the ITU-R troposcatter propagation model is not suitable for modeling fast variations in channels and scattering mechanism owing to its statistical and empirical methods. Therefore, theoretical models are used to model the effects of air turbulence and scattering mechanism.

In [3], new troposcatter transmission loss prediction model from troposcatter mechanism aspect was proposed. Three main theories of the troposcatter mechanism were introduced : turbulent incoherent scattering theory [16], coherent reflection by stable layers theory [17], and incoherent reflection by irregular layers theory [18]. Then, the troposcatter transmission loss expression based on three scattering mechanisms was determined. The particle swarm optimization algorithm was used to determine the weighting factors of loss. The weighting factors were determined differently depending on the climate zone of ITU-R model. To verify the proposed model, the authors compared the prediction results with three ITU-R models. In climate zones 4 and 5, the new prediction model was more accurate than P.617 and P.2001, and similar to P.452. In climate zone 6, the new prediction model was more accurate than the three ITU-R models.

In [13], a novel ray-based multiple-input–multiple-output (MIMO) channel model was proposed for b-LoS communication, along with a scattering cross-section model and differential radar range equation calculation. A ray-based technique was used to predict the propagation loss, and variations in the air turbulence were modeled using Kolmogorov theory. Additionally, variations in the common volume owing to changes in the refractive index of the troposphere were considered. The refractivity was calculated using two methods: using the temperature and vapor pressure of the real-world data set or using the ITU-R refractivity model of [26]. In addition, the transmission loss, coherence bandwidth, root mean square delay spread, and vertical correlation of the proposed model were analyzed. To justify the ray-based approach, studies have also compared their transmission losses with that of the troposcatter channel model of P.617. The experimental environment for such comparisons was described in [37], and the average refractivity calculation method of [26] has been used for the refractivity profile. When the model proposed in [13] was compared to the channel model of P.617, the troposcatter loss of the proposed model was shown to be similar to that of P.617 at a time percentage of 50%.

3.3. Ray tracing and parabolic equation method

This subsection provides a review of recent studies on ray path tracing methods for troposcatter channel modeling. The ray tracing method can be applied to channel modeling by predicting the path of the rays and comparing it with the measurement data. To trace the path of rays accurately, it is important to trace the refractive index gradient according to the altitude. In long-distance propagation environments, most ray path prediction methods use two methods: geometrical optics ray tracing or the parabolic equation method. It is known that the parabolic equation method is more appropriate in long-range and narrow environments, such as in tropospheric propagation [38].

In [39], a refractivity profile modeling method was proposed according to the altitude and parameters of the ray refraction path geometry. A geometrical optics ray-tracing method was used to simulate the elevated duct refractivity profile and normal refractivity profile. According to the launch angle of the transmitted signal, the results regarding the height of arrival, excess path length, absolute angle of arrival, and relative amplitude of the received signal were analyzed. Additionally, the amplitude, angle of arrival (AOA), and relative path delay changes according to the received height were compared. Consequently, the signals received at the receiver placed within the duct consisted of three paths with significantly different characteristics according to the signal received in the normal profile. Furthermore, if the launch angle changed, an odd number of ray paths arrived at the receiver.

In [40], a troposcatter mechanism was analyzed using the parabolic equation, and a tropospheric scatter model was proposed using the parabolic equation portion of the radio physical optics(RPO) model. The parabolic equation method of the RPO model is concluded to be better than the Engineer's

Table 4
Comparison of Literature and ITU-R Models.

Ref.	Contribution	Compared with ITU-R Model
[20]	ITU-R P.617, P.2001 and P.452 were combined to propose a new troposcatter transmission loss model using genetic algorithm optimizations.	The mean value and root mean square error of the new proposed model were compared against those of the three independent ITU-R models.
[32]	The ITU-R troposcatter model did not consider deviation loss so the authors derived the troposcatter deviation loss.	Not compared to the ITU-R model.
[35]	A non-uniform rain attenuation model was developed for troposcatter communications.	Comparison with the ITU-R rectangular and uniform rain cell model.
[3]	The troposcatter transmission loss expression based on three scattering mechanisms [16–18] was determined using particle swarm optimization.	Compare the errors relative to actual loss with three ITU-R models.
[13]	A ray-based technique was used to predict the propagation loss, and variations in air turbulence were modeled using Kolmogorov theory.	Compare troposcatter loss prediction with the ITU-R P.617 model.
[39]	A refractivity profile modeling method was proposed according to the altitude.	Not compared to the ITU-R model.
[40]	A troposcatter mechanism was analyzed using the parabolic equation.	Not compared to the ITU-R model.
[42]	Finite differences and Fourier transform implementations were used to numerically solve the parabolic equation.	Not compared to the ITU-R model.
[43]	The parabolic equation method used two implementations: split-step Padé and split-step Fourier approaches.	Not compared to the ITU-R model.

refractive effects prediction system (EREPS) method. A drawback of the troposcatter model using EREPS is the addition of a significant computational burden as the model must be evaluated at all ranges and elevations, in parallel with the parabolic equation model to add the scattering results. The measurement data used for the analysis were presented in [41]. The experimental results showed that the RPO-scatter model was more similar to the measurement data than the EREPS and RPO without a scatter model.

In [42], a tropospheric refraction modeling approach using both the ray-tracing and parabolic equation methods was proposed. For the parabolic equation method, the finite differences and Fourier transform implementations used to numerically solve the parabolic equation, were briefly described. Moreover, a calculation of the AOA was proposed for multipath propagation simulations.

In [43], the tropospheric propagation was also modeled using both the ray-tracing method and parabolic equation method, and was compared to actual measurement data. The measurement data considered the AOA and received the signal amplitude at a 50 km link in Ontario. The refractivity gradient modeling and ray-tracing method were the same as in [39]. The parabolic equation method used two implementations: split-step Padé and split-step Fourier approaches. The refractivity profile assumed three environments: a standard atmospheric gradient, ground-based layer, and elevated duct.

Table 4 summarizes the contribution of the research reviewed in Sections 3.1 to 3.3. Some studies provide the comparison of troposcatter loss prediction results with the ITU-R model, and the brief descriptions of the comparison are also summarized in Table 4.

3.4. Other research

In [6], cognitive scenarios and cognitive system architectures were proposed for troposcatter transceivers. Two cognitive scenarios were assumed: one for a troposcatter receiver, and the other for a troposcatter transmitter. In both scenarios, the troposcatter systems coexisted with satellite–terrestrial terminals and microwave terminals. The troposcatter communication acted as a secondary link when the troposcatter transceivers accessed the licensed spectra of satellite or terrestrial microwave users.

In [44], a transfer function for troposcatter channels was derived based on the scattering field and a closed-form expression of the coherence bandwidth for the troposcatter links. Subsequently, the derived equations and experimental measurements were compared. Measurement data of the median coherence bandwidths were obtained using the results of four different troposcatter paths: the Ontario Center, Whitford Field, Point Petre, and Port Byron paths [45]. As a result of the comparison, the derived formula could provide a more accurate prediction for longer troposcatter paths than for shorter ones. Moreover, the proposed coherence bandwidth formula could effectively characterize the frequency fading correlation characteristics.

4. Conclusion

Tropospheric scatter communication is a promising candidate for b-LOS communication owing to its low transmission delay and security robustness. In this study, we analyzed three propagation model for troposcatter recommended by the ITU-R. We investigated the differences between the three

troposcatter models and how the prediction loss in the real environment appears differently for each model through simulation. Additionally, further research on the ITU-R propagation model is reviewed. Studies on the novel troposcatter channel model and transmission loss prediction based on the theoretical model, which is a different approach from the empirical ITU-R model, was also reviewed. We reviewed troposcatter channel models using the ray tracing and the parabolic equation method. Finally, studies on troposcatter communication were also reviewed. To implement a troposcatter communication system, troposcatter channel modeling is crucial. Since the performance of the communication varies depending on the location of the common volume, refractive index, and atmospheric conditions, as well as on communication parameters such as the distance and frequency, various parameters must be appropriately considered in the troposcatter channel model.

Declaration of competing interest

The authors declare that they have no known competing financial interests or personal relationships that could have appeared to influence the work reported in this paper.

Acknowledgments

This work was supported by the Nuclear Safety Research Program through the Korea Foundation Of Nuclear Safety (KoFONS) using the financial resource granted by the Nuclear Safety and Security Commission (NSSC) of the Republic of Korea (No. 1805006).

References

[1] E. Dinc, O.B. Akan, A ray-based channel model for MIMO troposcatter communications, in: 2013 IEEE 24th Annual International Symposium on Personal, Indoor, and Mobile Radio Communications (PIMRC), 2013, pp. 243–247, http://dx.doi.org/10.1109/PIMRC.2013.6666139.

[2] E. Dinc, O.B. Akan, Fading correlation analysis in MIMO-OFDM troposcatter communications: Space, frequency, angle and space-frequency diversity, IEEE Trans. Commun. 63 (2) (2015) 476–486, http://dx.doi.org/10.1109/TCOMM.2014.2387159.

[3] D. Yuan, X. Chen, Troposcatter transmission loss prediction based on particle swarm optimisation, IET Microw. Antennas Propag. 15 (3) (2021) 332–341, http://dx.doi.org/10.1049/mia2.12052, arXiv:https://ietresearch.onlinelibrary.wiley.com/doi/pdf/10.1049/mia2.12052. URL https://ietresearch.onlinelibrary.wiley.com/doi/abs/10.1049/mia2.12052.

[4] Z. Liu, X. Chen, C. Li, Q. Liu, Research on detection performance of passive detection system based on troposcatter, AEU - International Journal of Electronics and Communications 95 (2018) 170–176, http://dx.doi.org/10.1016/j.aeue.2018.08.008, URL https://www.sciencedirect.com/science/article/pii/S1434841118305508.

[5] X. Mi, Z. Liu, X. Chen, Q. Liu, An efficient DOA estimation method for passive surveillance system based on troposcatter, Math. Probl. Eng. 2021 (2021) 7, http://dx.doi.org/10.1155/2021/6650278.

[6] C. Li, X. Chen, X. Liu, Cognitive tropospheric scatter communication, IEEE Trans. Veh. Technol. 67 (2) (2018) 1482–1491, http://dx.doi.org/10.1109/TVT.2017.2761440.

[7] E. Dinc, O.B. Akan, More than the eye can see: Coherence time and coherence bandwidth of troposcatter links for mobile receivers, IEEE Veh. Technol. Mag. 10 (2) (2015) 86–92, http://dx.doi.org/10.1109/MVT.2015.2410786.

[8] Introduction to Troposcatter Communications, a Brief Synopsis of Over-The-Horizon Troposcatter, Technical Information, Comtech Systems, Inc, 2009.

[9] I. Nadeem, M. Alibakhshikenari, F. Babaeian, A. Althuwayb, B. Virdee, L. Azpilicueta, S. Khan, I. Huynen, F. Falcone, T. Denidni, E. Limiti, A comprehensive survey on “circular polarized antennas” for existing and emerging wireless communication technologies, J. Phys. D: Appl. Phys. 55 (2021) http://dx.doi.org/10.1088/1361-6463/ac2c36.

[10] M. Alibakhshikenari, Design and modeling of new UWB metamaterial planar cavity antennas with shrinking of the physical size for modern transceivers, Int. J. Antennas Propag. 2013 (2013) http://dx.doi.org/10.1155/2013/562538.

[11] M. Alibakhshikenari, M. Naser-Moghadasi, R. Sadeghzadeh, B. Virdee, E. Limiti, New CRLH-based planar slotted antennas with helical inductors for wireless communication systems, RF-circuits and microwave devices at UHF-SHF bands, Wirel. Pers. Commun. 92 (2017) http://dx.doi.org/10.1007/s11277-016-3590-4.

[12] M. Alibakhshikenari, M. Naser-Moghadasi, R. Sadeghzadeh, B. Virdee, E. Limiti, New compact antenna based on simplified CRLH-TL for UWB wireless communication systems, Int. J. RF Microw. Comput.-Aided Eng. 26 (2016) n/a–n/a, http://dx.doi.org/10.1002/mmce.20956.

[13] E. Dinc, O.B. Akan, A ray-based channel modeling approach for MIMO troposcatter beyond-line-of-sight (b-LoS) communications, IEEE Trans. Commun. 63 (5) (2015) 1690–1699, http://dx.doi.org/10.1109/TCOMM.2015.2416716.

[14] S. Zhang, X.-H. Chen, Q. Liu, X.-P. Mi, A new model for estimating troposcatter loss and delays based on ray-tracing and beam splitting with ERA5, IEEE Trans. Antennas and Propagation 70 (7) (2022) 5770–5783, http://dx.doi.org/10.1109/TAP.2022.3161458.

[15] M.A. Rupar, E. Larsen, H.B. Saglam, J.A. Savin, B. Gurdil, T.A. Lampe, N. Bruck, S. Peltotalo, R.B. Blasco, Airborne beyond line-of-sight communication networks, IEEE Commun. Mag. 58 (8) (2020) 34–39, http://dx.doi.org/10.1109/MCOM.001.2000307.

[16] H. Booker, W. Gordon, A theory of radio scattering in the troposphere, Proc. IRE 38 (4) (1950) 401–412, http://dx.doi.org/10.1109/JRPROC.1950.231435.

[17] K. Bullington, Reflections from an exponential atmosphere, Bell Syst. Tech. J. 42 (6) (1963) 2849–2867, http://dx.doi.org/10.1002/j.1538-7305.1963.tb00989.x.

[18] H.T. Friis, A.B. Crawford, D.C. Hogg, A reflection theory for propagation beyond the horizon, Bell Syst. Tech. J. 36 (3) (1957) 627–644, http://dx.doi.org/10.1002/j.1538-7305.1957.tb03856.x.

[19] Data banks used for testing prediction methods, 1986, CCIR document 370-5.

[20] L. Li, Z.-S. Wu, L.-K. Lin, R. Zhang, Z.-W. Zhao, Study on the prediction of troposcatter transmission loss, IEEE Trans. Antennas and Propagation 64 (3) (2016) 1071–1079, http://dx.doi.org/10.1109/TAP.2016.2515125.

[21] Prediction procedure for the evaluation of interference between stations on the surface of the earth at frequencies above about 0.1 GHz, 2021, ITU-R Recommendation P.452-17.

[22] Propagation prediction techniques and data required for the design of trans-horizon radio-relay systems, 2019, ITU-R Recommendation P.617-5.

[23] A general purpose wide-range terrestrial propagation model in the frequency range 30 MHz to 50 GHz, 2021, ITU-R Recommendation P.2001-4.

[24] Characteristics of precipitation for propagation modeling recommendation, 2007, ITU-R Recommendation P.837-5.

[25] L. Luini, L. Emiliani, X. Boulanger, C. Riva, N. Jeannin, Rainfall rate prediction for propagation applications: Model performance at regional level over Ireland, IEEE Trans. Antennas and Propagation 65 (11) (2017) 6185–6189, http://dx.doi.org/10.1109/TAP.2017.2754448.

[26] The radio refractive index: its formula and refractivity data, 2019, ITU-R Recommendation P.453-14.

[27] Propagation data and prediction methods required for the design of earth-space telecommunication systems, 2017, ITU-R Recommendation P.618-13.

[28] Attenuation by atmospheric gases and related effects, 2019, ITU-R Recommendation P.676-12.
[29] Reference standard atmospheres, 2017, ITU-R Recommendation P.835-6.
[30] Attenuation due to clouds and fog, 2019, ITU-R Recommendation P.840-8.
[31] Guide to the application of the propagation methods of radiocommunication study group 3, 2021, ITU-R Recommendation P.1144-11.
[32] Z. Wang, M. Wang, Troposcatter deviation losses study for OTH microwave propagation, IEEE Trans. Antennas and Propagation 66 (12) (2018) 6476–6481, http://dx.doi.org/10.1109/TAP.2018.2879777.
[33] J.H. Chisholm, P.A. Portmann, J.T. deBettencourt, J.F. Roche, Investigations of angular scattering and multipath properties of tropospheric propagation of short radio waves beyond the horizon, Proc. IRE 43 (10) (1955) 1317–1335, http://dx.doi.org/10.1109/JRPROC.1955.277945.
[34] D. Cox, A. Waterman, Phase and amplitude measurements of transhorizon microwaves: Angular response patterns in elevation, IEEE Trans. Antennas and Propagation 19 (2) (1971) 262–273, http://dx.doi.org/10.1109/TAP.1971.1139901.
[35] E. Dinc, O.B. Akan, A nonuniform spatial rain attenuation model for troposcatter communication links, IEEE Wirel. Commun. Lett. 4 (4) (2015) 441–444, http://dx.doi.org/10.1109/LWC.2015.2433261.
[36] L. Féral, H. Sauvageot, L. Castanet, J. Lemorton, HYCELL—A new hybrid model of the rain horizontal distribution for propagation studies: 1. Modeling of the rain cell, Radio Sci. 38 (3) (2003) http://dx.doi.org/10.1029/2002RS002802.
[37] NAMMA lidar atmospheric sensing experiment (LASE), nat. Aeronautics space admin. (NASA) EOSDIS GHRC DAAC, Washington, DC, USA, 2013, [Online]. Available: http://ghrc.msfc.nasa.gov/index.html.
[38] Z. Yun, M.F. Iskander, Ray tracing for radio propagation modeling: Principles and applications, IEEE Access 3 (2015) 1089–1100, http://dx.doi.org/10.1109/ACCESS.2015.2453991.
[39] A. Webster, Raypath parameters in tropospheric multipath propagation, IEEE Trans. Antennas and Propagation 30 (4) (1982) 796–800, http://dx.doi.org/10.1109/TAP.1982.1142840.
[40] H. Hitney, A practical tropospheric scatter model using the parabolic equation, IEEE Trans. Antennas and Propagation 41 (7) (1993) 905–909, http://dx.doi.org/10.1109/8.237621.
[41] L.A. Ames, P. Newman, T.F. Rogers, VHF tropospheric overwater measurements far beyond the radio horizon, Proc. IRE 43 (10) (1955) 1369–1373, http://dx.doi.org/10.1109/JRPROC.1955.277950.
[42] P. Valtr, P. Pechac, Tropospheric refraction modeling using ray-tracing and parabolic equation, Radioengineering 14 (2005).
[43] R. Akbarpour, A. Webster, Ray-tracing and parabolic equation methods in the modeling of a tropospheric microwave link, IEEE Trans. Antennas and Propagation 53 (11) (2005) 3785–3791, http://dx.doi.org/10.1109/TAP.2005.856355.
[44] C. Li, X. Chen, Z. Xie, A closed-form expression of coherence bandwidth for troposcatter links, IEEE Commun. Lett. 22 (3) (2018) 646–649, http://dx.doi.org/10.1109/LCOMM.2017.2785850.
[45] D. Kennedy, A comparison of measure and calculated frequency correlation functions over 4.6- and 7.6-GHz troposcatter paths, IEEE Trans. Commun. 20 (2) (1972) 173–178, http://dx.doi.org/10.1109/TCOM.1972.1091148.